Supplementary Information

Title: Loss of BAP1 function leads to EZH2-dependent transformation

Authors: Lindsay M. LaFave, Wendy Béguelin, Richard Koche, Matt Teater, Barbara Spitzer, Alan Chramiec, Efthymia Papalexi, Matthew D. Keller, Todd Hricik, Katerina Konstantinoff, Jean-Baptiste Micol, Benjamin Durham, Sarah K. Knutson, John E. Campbell, Gil Blum, Xinxu Shi, Emma H. Doud, Andrei V. Krivtsov, Young Rock Chung, Inna Khodos, Elisa de Stanchina, Ouathek Ouerfelli, Prasad S. Adusumilli, Paul M. Thomas, Neil L. Kelleher, Minkui Luo, Heike Keilhack, Omar Abdel-Wahab, Ari Melnick, Scott A. Armstrong, Ross L. Levine

Primers

	Genotyping Primers (mouse)
Bap1 up	Actgcagcaatgtggatctg
Bap1 down	Gaaaaggtctgacccagatca
Bap1 flox F	Gcgcaacgcaattaatgata
Bap1 flox R	Cagtgtccagaatggctcaa

	Mutagenesis Primers (human)
BAP1 C91A sense	ccaccagctgatacccaactctgctgcaactcatgc
BAP1 C91A antisense	gcatgagttgcagcagagttgggtatcagctggtgg

	Mouse qPCR Primers
Ezh2 F	AGCACAAGTCATCCCGTTAAAG
Ezh2 R	AATTCTGTTGTAAGGGCGACC
Suz12 F	GGCTGACCACGAGCTTTTC
Suz12 R	TGGTGCGATAAGATTTCGAGTTC
Bap1 F	GTTGGTGGATGACACGTCTG
Bap1 R	CTCAGGACTGAAGCCTTTGG
Actin B F	GATCTGGCACCACACCTTCT
Actin B R	CCATCACAATGCCTGTGGTA
HoxA5 F	GCTCAGCCCCAGATCTACC
HoxA5 R	GGCATGAGCTATTTCGATCC
HoxA6 F	CCCTGTTTACCCCTGGATG
HoxA6 R	ACCGACCGGAAGTACACAAG
HoxA8 F	CTTCTCCAGTTCCAGCGTCT
HoxA8 R	AGGTAGCGGTTGAAATGGAA
HoxA9 F	ATGCTTGTGGTTCTCCTCCA
HoxA9 R	GTTCCAGCGTCTGGTGTTTT

	Human qPCR Primers
E-CAD F	GACCGGTGCAATCTTCAAA
E-CAD R	TTGACGCCGAGAGCTACAC
HPRT F	CATTATGCCGAGGATTTGG
HPRT R	GCAAGTCTTTCAGTCCTGT
BAP1 F	CGATCCATTTGAACAGGAAGA
BAP1 R	CTCGTGGAAGATTTCGGTGT

	ChIP qPCR primers (human)
EZH2-1 F	AGCTGACTCAAGCTGCTTGT
EZH2-1 R	CAGGAAACCTGAGATTTTCA
MORC3 F	catcttccccaagctcccaat
MORC3 R	GAGCGAGCTACAAAGCCAGGA
E2F6 F	cctgttcccttcctctggaa
E2F6 R	cgacgcagacggaaaaagag
PHF20 F	tgagtggggacttcgtgttc
PHF20 R	gaccaaccgacagaaggact
JAM2 F	tccacccctaggctgaaaag
JAM2 R	gatcggctttgtgtctggtc

Supplementary Table 1. Primer Sequences

Supplementary Figure 1

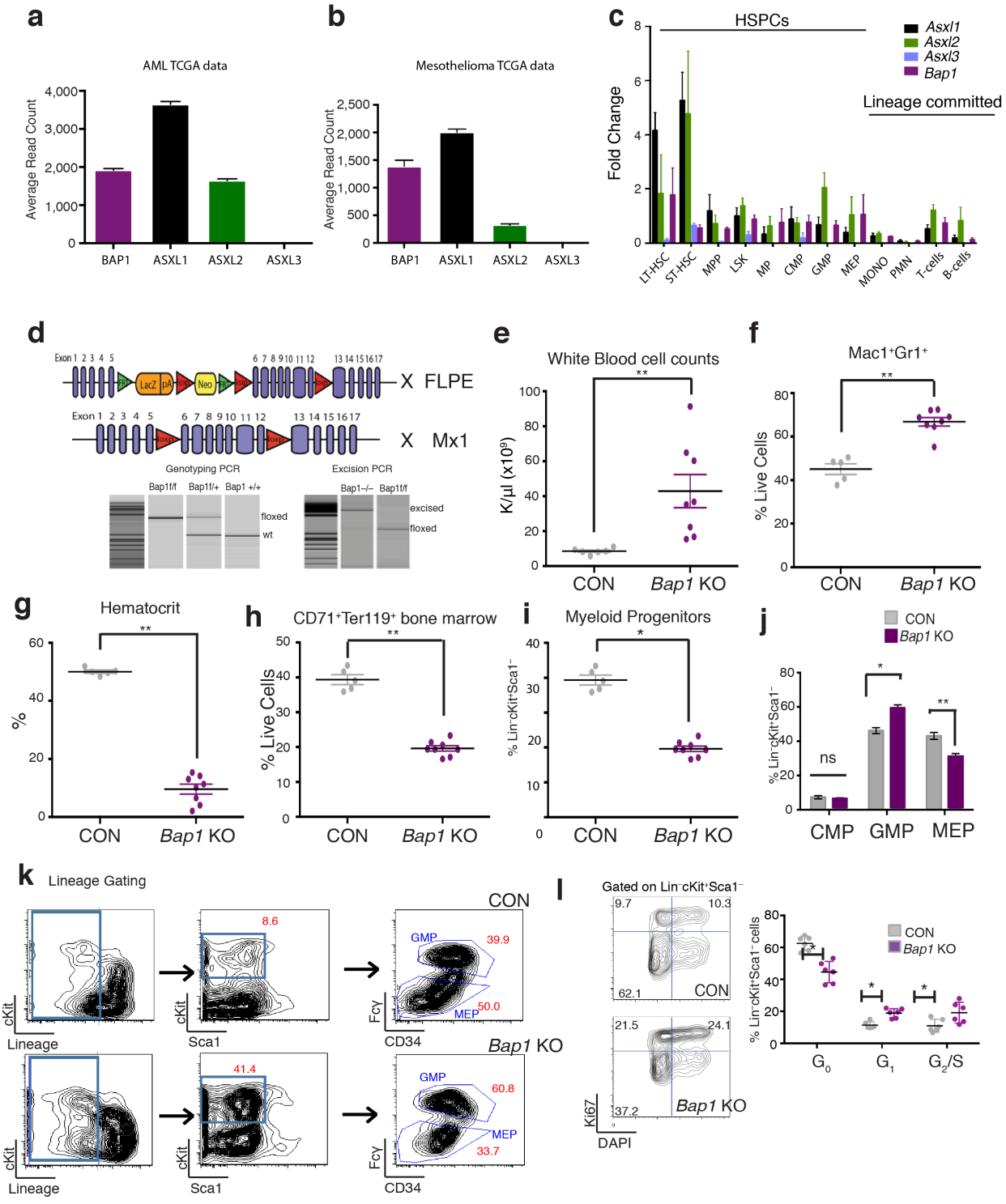

Supplementary Figure 1. Characterization of conditional hematopoietic deletion of *Bap1.* (**a**) Average gene expression of BAP1, ASXL1, ASXL2, and ASXL3 in TCGA AML (acute myeloid leukemia) and (**b**) mesothelioma patients as expressed as a mathematical mean with standard error of normalized read counts. (**c**) *Bap1* expression by qRT-PCR in purified populations of hematopoietic cells in C57/B6H mice. LT-HSC, long term hematopoietic stem cells (HSCs) ($Lin^-Sca\text{-}1^+c\text{-}Kit^+CD150^+CD48^-$); ST-HSC, short term HSCs ($Lin^-Sca\text{-}1^+c\text{-}Kit^+CD150^+CD48^+$); MPP, mulitpotent progenitor ($Lin^-Sca\text{-}1^+c\text{-}Kit^+CD150^-CD48^+$); LSK, $Lin^-Sca\text{-}1^+c\text{-}Kit^+$; MP, myeloid progenitors ($Lin^-Sca\text{-}1^-c\text{-}Kit^+$); GMP, Granulocyte Macrophage Progenitors ($Lin^-Sca\text{-}1^-c\text{-}Kit^+$ $CD34^+FcY^+$); CMP, Common Myeloid Progenitors ($Lin^-Sca\text{-}1^-c\text{-}Kit^+$ $CD34^+FcY^{lo}$); MEP, Macrophage Erythroid Progenitors ($Lin^-Sca\text{-}1^-c\text{-}Kit^+$ $CD34^-FcY^-$); MONO, monocytes ($Mac1^+Gr1^-$); PMN, (polymorphonuclear neutrophil, $Mac1^+Gr1^+$); T cells, $CD3^+$; and B cells, $B220^+$. (**d**) *Bap1* targeting scheme in murine embryonic stem cells obtained from the EUCOMM consortium. After chimera generation, mice were crossed with transgenic FLPE mice to excise the premature stop cassette. Mice were then crossed to Mx1-*Cre* transgenic mice. Genotyping schemes confirming genotype and excision 4 weeks post-polyIpolyC (pIpC) treatment. (**e**) Enumeration of white blood cells in peripheral blood in control and *Bap1* KO mice after treatment with (pIpC) to induce excision and (**f**) flow cytometric enumeration of myeloid cells ($Mac1^+Gr1^+$). (**g**) Hematocrit percentages in peripheral blood and (**h**) flow cytometric enumeration of red blood cell precursors ($CD71^+Ter119^+$) in control and *Bap1* KO mouse bone marrow after pIpC-induced excision. (**i**) Relative frequencies of control and *Bap1* KO bone marrow myeloid progenitor populations ($Lin^-c\text{-}Kit^+Sca\text{-}1^-$). Cells were gated on live lineage-negative populations. (**j**) Relative quantification of bone marrow myeloid progenitor cell populations (GMP, CMP, MEP) in control and *Bap1* KO mice. (**k**) Flow plots from example control and bone marrow animals to demonstrate progenitor and GMP expansion. (**l**) Flow cytometric enumeration of cycling progenitor cells (Ki67/DAPI stain); for all experiments: *n* = 5 CON mice and *n* = 8 *Bap1* KO mice.

Supplementary Figure 2

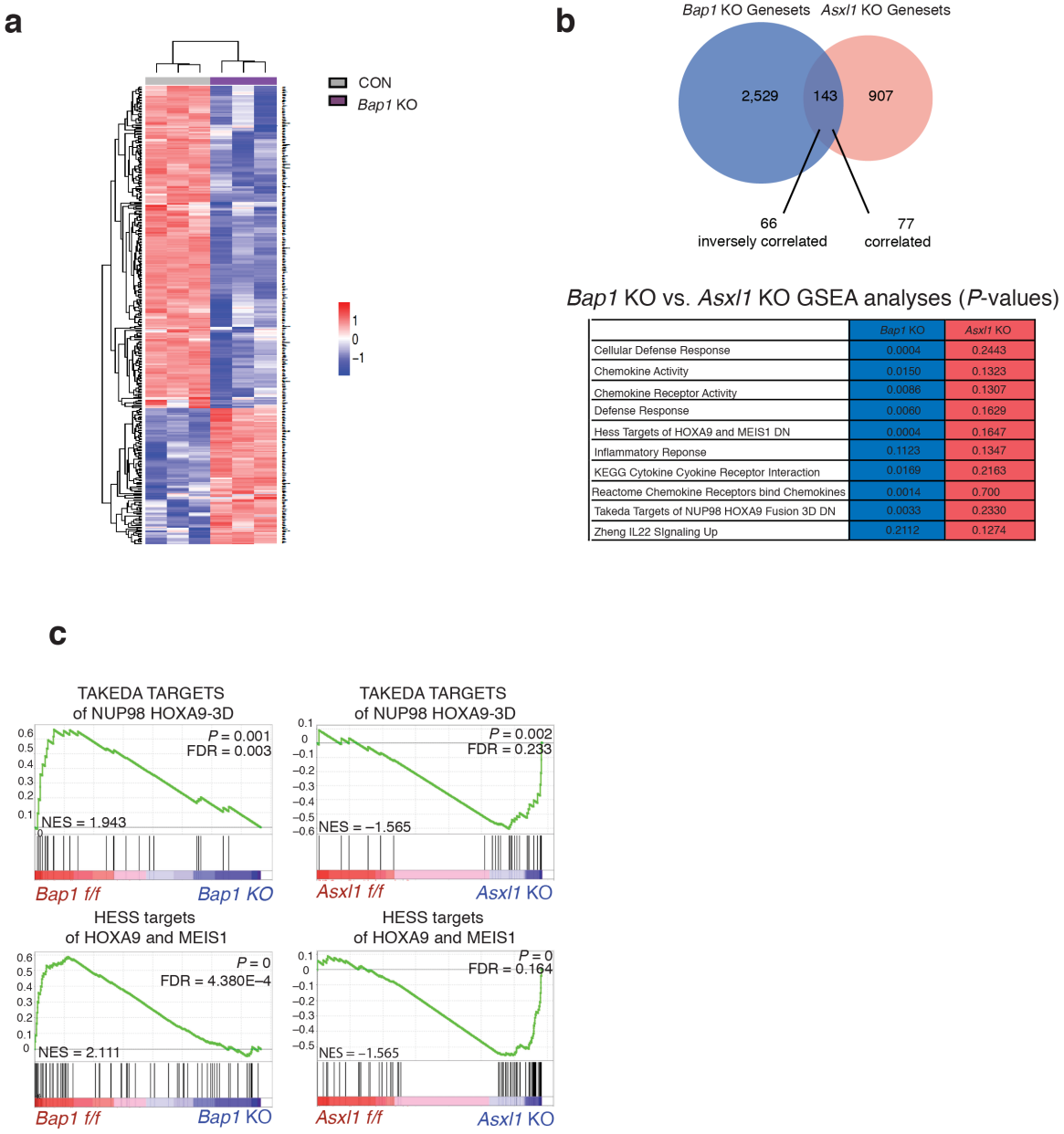

Supplementary Figure 2. *Bap1* and *Asxl1* loss results in opposing gene expression changes. (**a**) RNA-Seq data of differentially expressed genes in control versus *Bap1* KO mice

granulocyte-macrophage progenitors (GMPs; $Lin^{-}c\text{-}Kit^{+}Sca1^{-}CD34^{+}$ $Fc\gamma^{+}$); cells analyzed with DESeq2 (cutoff *P*-value $P < 0.05$). Heatmap indicates genes increasing (red) and decreasing (blue) in expression. (**b**) Number of positively and negatively enriched genesets from the *Bap1* KO and *Asxl1* KO GSEA analysis hitting an FDR < 0.25 (top). Venn diagram depicting gene sets that are oppositely enriched in *Bap1* KO and *Asxl1* KO myeloid progenitors by RNA-Seq (bottom). (**c**) GSEA of oppositely enriched and statistically significant *HoxA* cluster gene sets in *Bap1* KO and *Asxl1* KO progenitor cells. *P*-values and FDR values are indicated.

Supplementary Figure 3

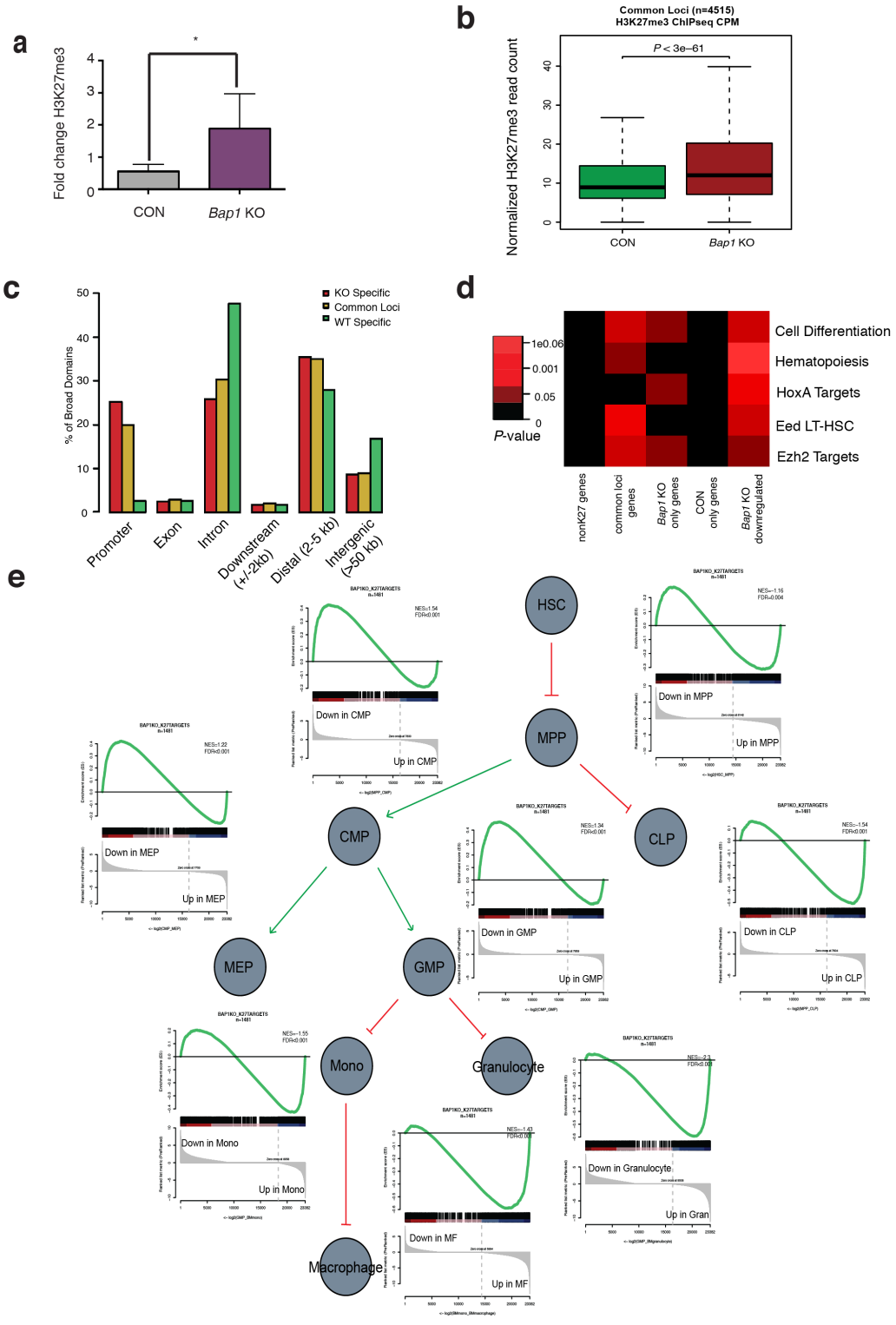

Supplementary Figure 3. Bap1 deletion enhances PRC2 activity. (**a**) ELISA of H3K27me3 normalized to total H3 in histones purified from bone marrow cells from *Bap1* KO and control

mice. (**b**) Box plot showing normalized H3K27me3 reads in c-Kit enriched bone marrow (*n* = 2). (**c**) Percentage of H3K27me3-broad domains called in relation to gene transcriptional start site (promoter, exon, intron, downstream (+/–2 kb), distal (2–5 kb), and intergeneic (> 50 kb)). 1 kb broad domain bins were analyzed across the genome and enriched regions were called as broad domains based on standard deviation over the mean. (**d**) GSEA demonstrating correlation of gene signatures to downregulated genes also marked with H3K27me3. (**e**) Published RNA-Seq from sorted bone marrow populations[1] was analyzed and compared to genes that were differentially downregulated and marked with H3K27me3 following *Bap1* loss were analyzed using GSEA. Genes that were downregulated and marked by H3K27me3 were only correlated with the hematopoietic progenitor populations, suggesting that these may be the relevant target populations. These data explain the progenitor expansion that we see in the *Bap1* KO mouse model.

Supplementary Figure 4

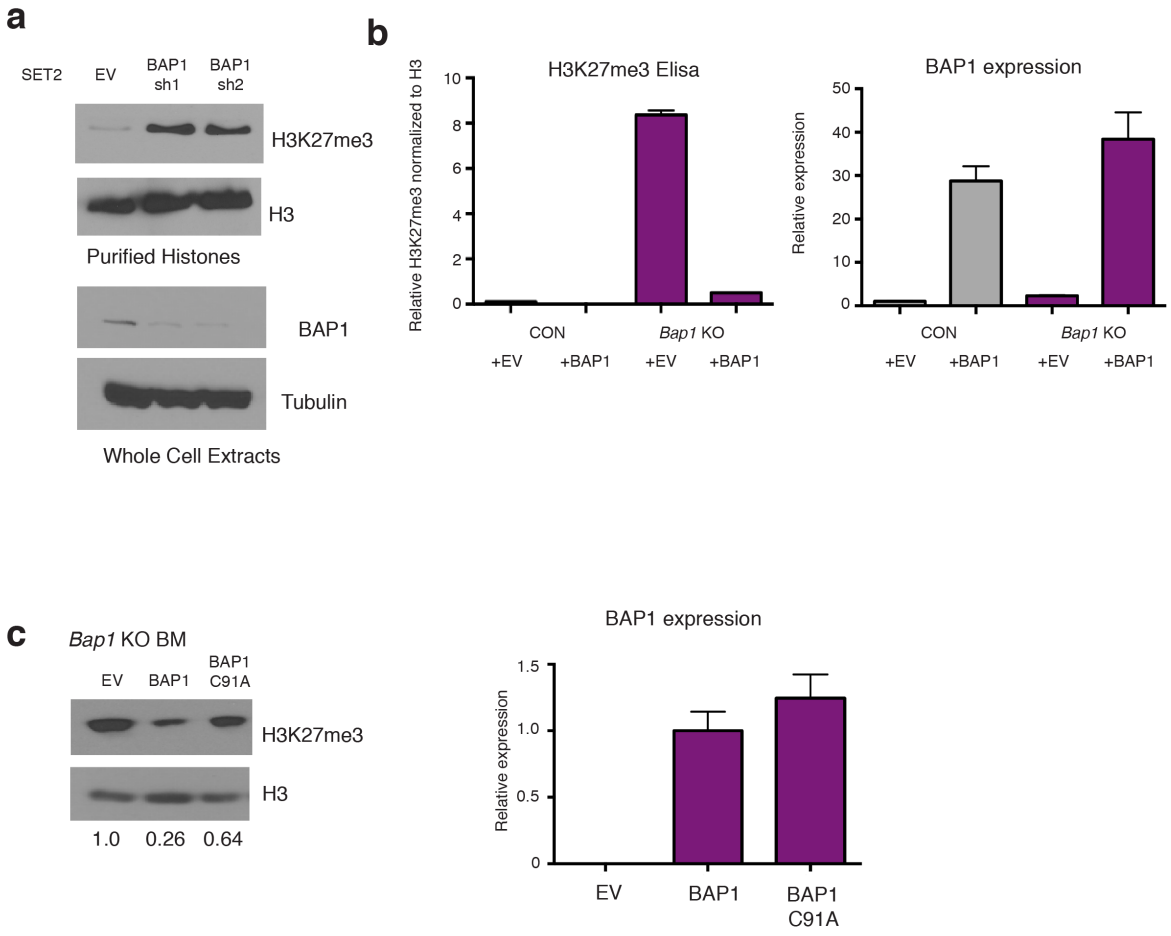

Supplementary Figure 4. *In vitro* BAP1 perturbations lead to changes in H3K27me3. (**a**) Western blot of SET2 cells transduced with two independent BAP1 shRNAs revealing H3K27me3 levels in purified histones and BAP1 knockdown from whole cell extract. (**b**) Methylcellulose assay with control and *Bap1* KO bone marrow cells. BAP1 cDNA constructs were reintroduced into control and Bap1 deleted cells. Histone ELISA assays were performed for H3K27me3. Quantitative qPCR to assess expression of BAP1 construct. (**c**) Reintroduction of BAP1 and deubiquitinase mutant *BAP1 C91A* in *Bap1*-deficient murine cells via transient transfection. Histone Western blots were performed for H3K27me3 and total H3. Densitometry conducted by ImageJ reported under western blot. Quantitative qPCR to show levels of construct expression. Normalized to cells with reintroduction of BAP1.

Supplementary Figure 5

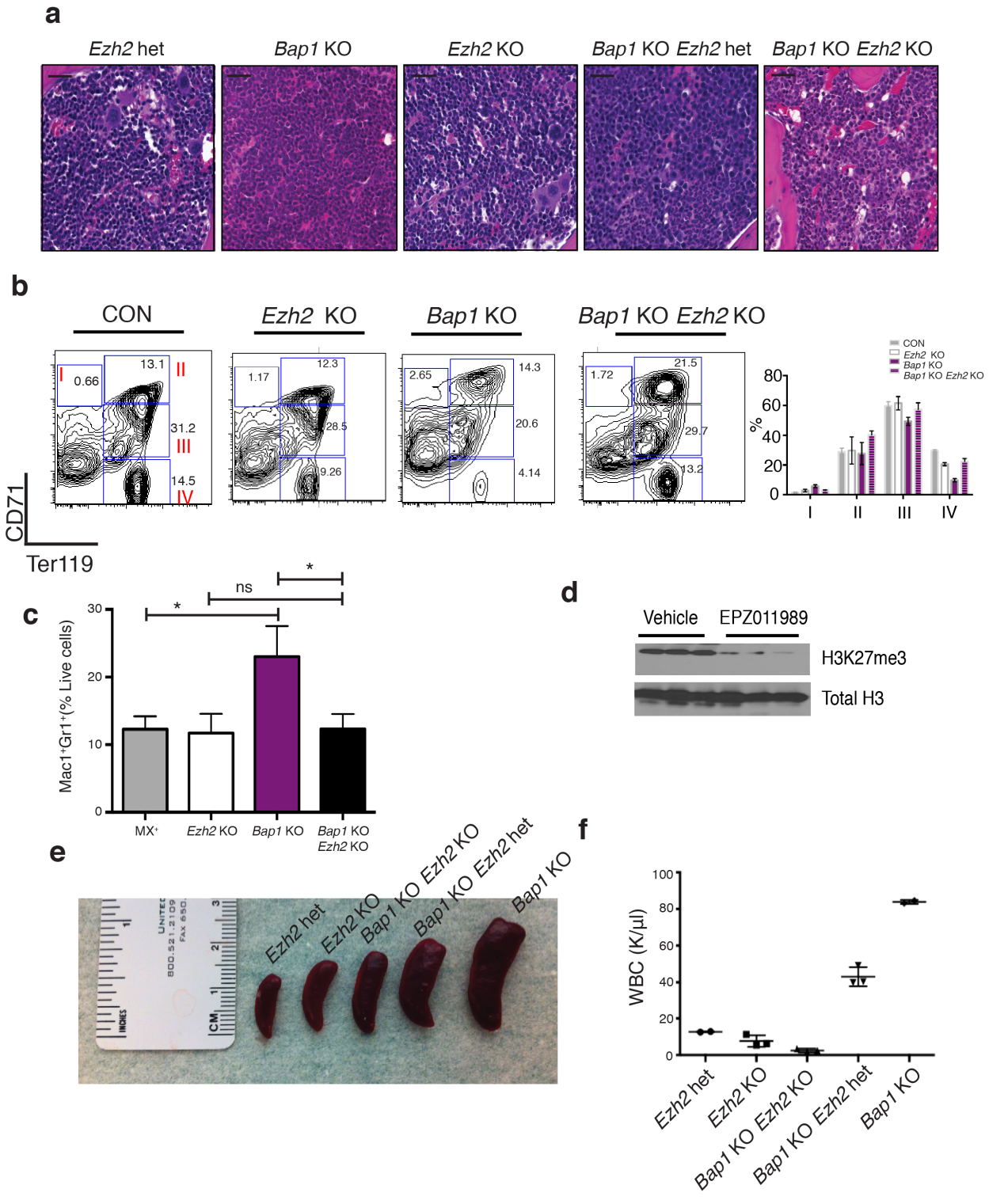

Supplementary Figure 5. Characterization of *Bap1*/*Ezh2* compound KO mice. (**a**) Bone marrow pathology for various *Bap1/Ezh2* genotypes, scale bar 100 μM. (**b**) Flow cytometric

staining for erythroid cells in indicated genotypes (CD71, Ter119) and quantification. (I-IV) are indicative of stages of erythroid differentiation with I being the most immature and IV being the most mature. Quantitation of these phenotypes on the right of the representative flow plots. (**c**) Percentage of $Mac1^{+}Gr1^{+}$ cells in indicated genotypes as enumerated by flow cytometry. (**d**) H3K27me3 levels in mice treated with either vehicle of EPZ011989 for 16 days (*n* = 3). (**e**) Spleen sizes for indicated genotypes, 4 weeks post-pIpC. (**f**) White blood cell counts for indicated genotypes, 4 weeks post-pIpC.

Supplementary Figure 6

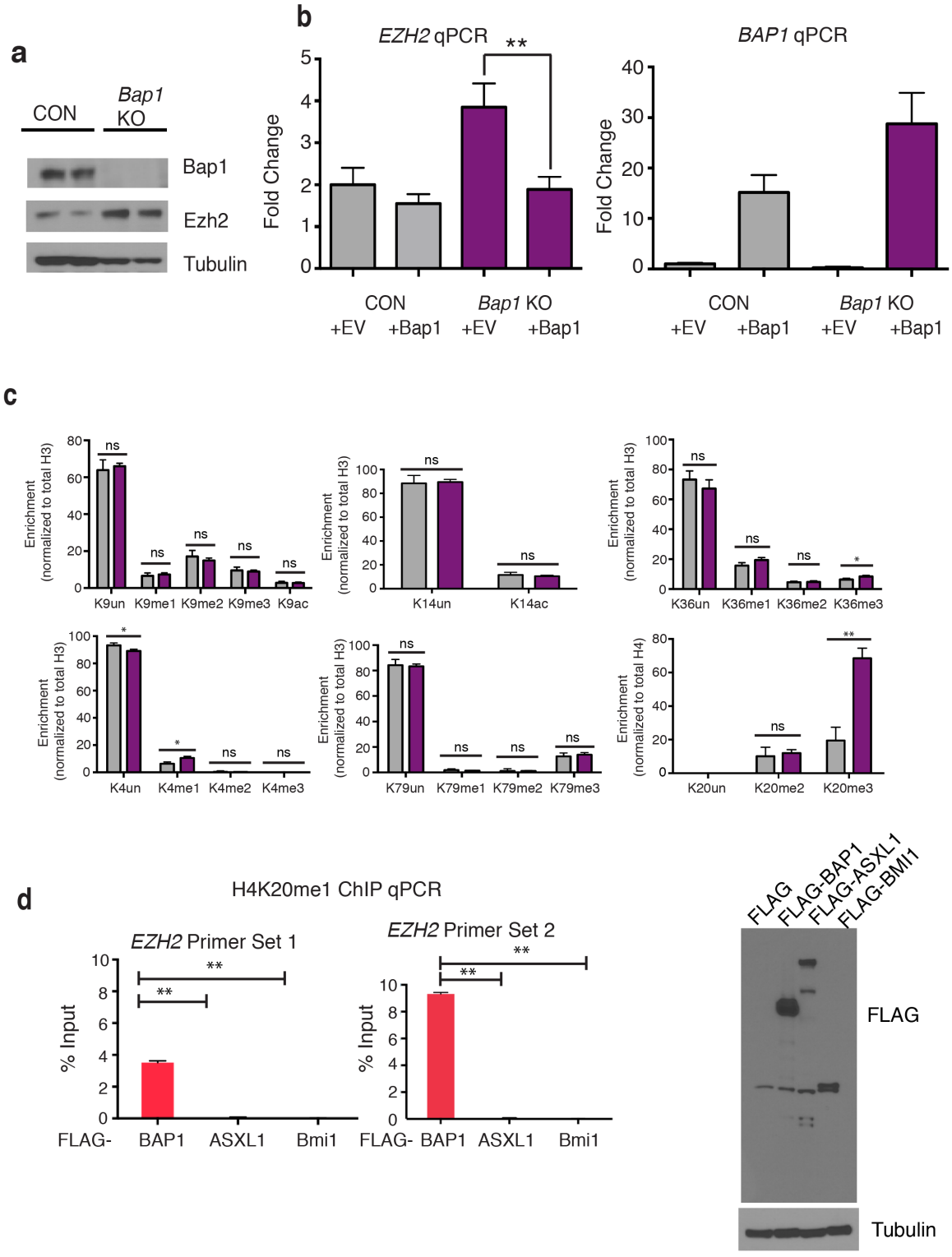

Supplementary Figure 6. Histone analyses in Bap1 KO animals. (**a**) EZH2 expression in Bap1 KO mouse bone marrow cells. (**b**) EZH2 transcription as assessed by qPCR in control and

Bap1 KO cells. Cells were either transduced with empty vector or a BAP1 overexpression construct. (**c**) Histone mass spectrometry in control and Bap1 KO animals c-Kit enriched bone marrow cells, *n* = 2. (**d**) H4K20me1 ChIP-qPCR experiments in 293T cells that overexpress FLAG-tagged BAP1, ASXL1 and Bmi1.

Supplementary Figure 7

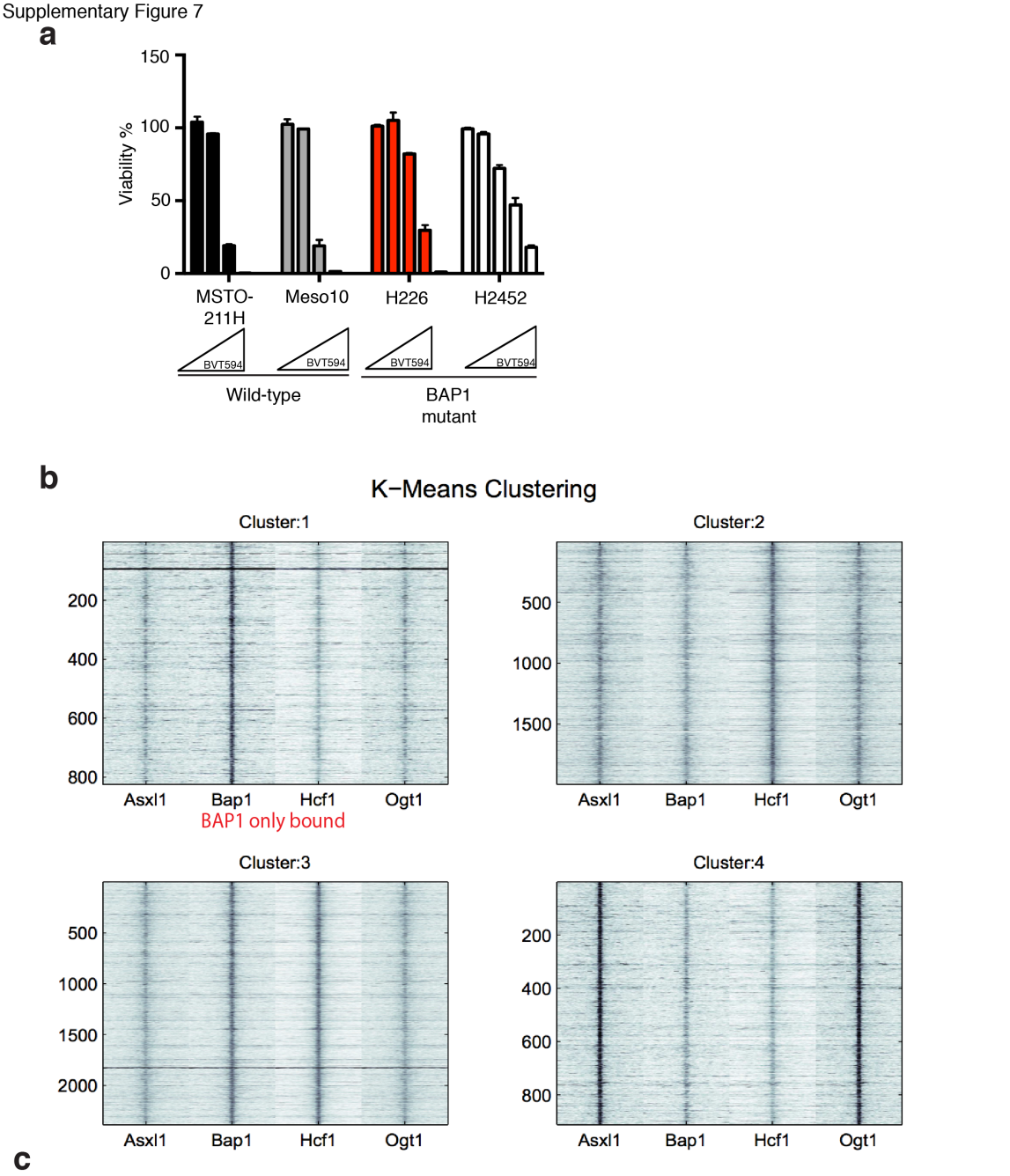

Supplementary Figure 7. Analysis of BAP1, ASXL1, HCF-1, and OGT binding. (**a**) Cell Titer Glo assay with 5, 10, or 20 μM of BVT594. (**b**) K-means clustering analyses for BAP1, ASXL1, HCF-1, and OGT ChIP-Seq. (**c**) Homer *de novo* motif analyses in BAP1-bound clusters.

Supplementary Figure 8

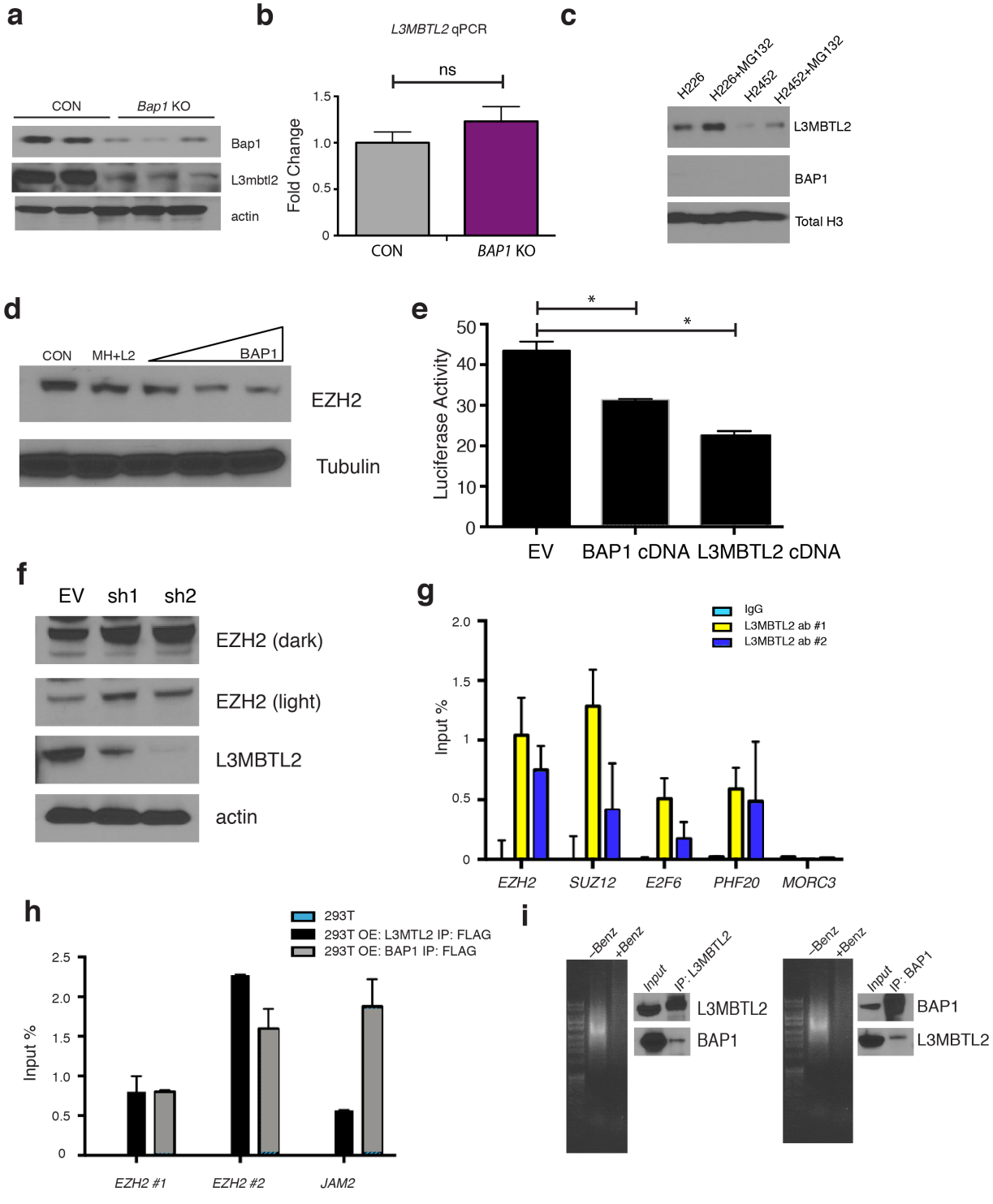

Supplementary Figure 8. L3MBTL2 and BAP1 co-regulate EZH2. (**a**) Expression of Bap1 and L3mblt2 in control and Bap1 KO bone marrow cells. (**b**) Expression of *L3mbtl2* by qPCR in GMPs. (**c**) Western blot of H226 and H2452 cells treated with 25 μM MG132. Insoluble fractions were extracted using 2% SDS containing lysis buffer. (**d**) Expression of EZH2 in cell lines overexpressing L3MBTL2. (**e**) EZH2 promoter activity assay with a construct containing 1.9 kB of the EZH2 promoter and a Renilla control vector transiently transfected into 293T cells with either empty vector, a BAP1 or L3MBTL2 expression vector. Firefly luciferase activity was normalized to Renilla activity in each of these conditions. (**f**) Two independent hairpins were used to knockdown L3MBTL2 protein in SET2 cells. Western blot analyses were conducted on L3MBTL2, EZH2, and actin including short and long exposures. (**g**) ChIP for *L3MBTL2* followed by qPCR at the *EZH2*, *SUZ12*, *E2F6* (positive control), *PHF20* (positive control), and *MORC3* (negative control) loci in 293T cells. (**h**) Anti-FLAG ChIP followed by qPCR at the *EZH2* locus in 293T cells overexpressing FLAG-L3MBTL2 or FLAG-BAP1. JAM2 is a positive control. Compared to 293T cells without FLAG overexpression. (**i**) Western blot for L3MBTL2 and BAP1 following respective IPs in 293T cells. Agarose DNA gel included to show DNA digestion.

Supplementary Figure 9

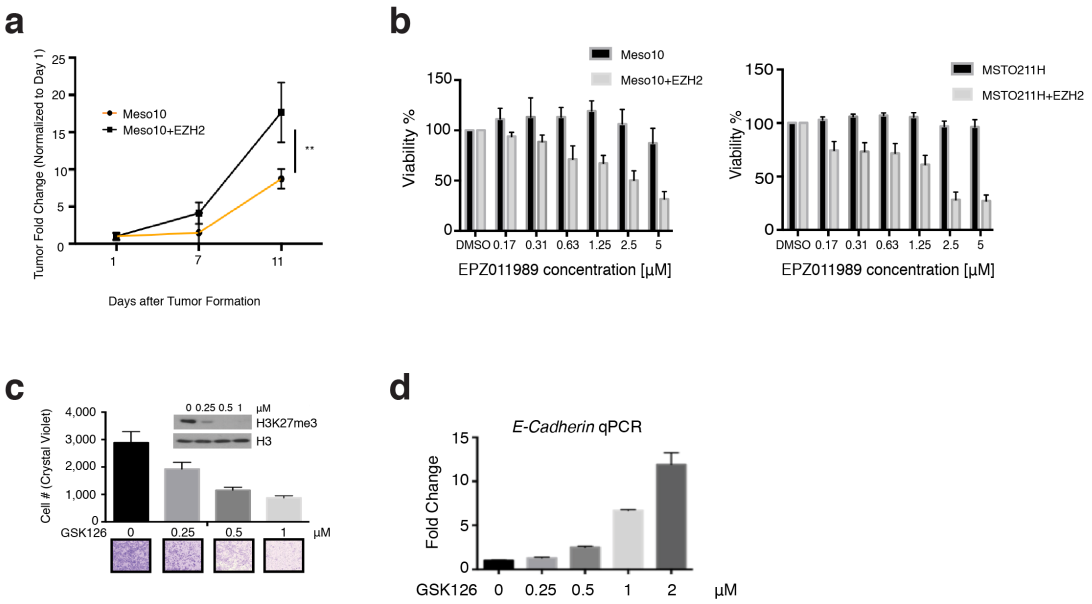

Supplementary Figure 9. BAP1 mutant cell lines are most sensitive to EZH2 inhibition. (**a**) Meso10 overexpressing cell lines increasingly proliferated when being injected into the flank of NOD-SCID mice. (**b**) EZH2 was overexpressed in MSTO-211H and Meso10 cell lines. The cell lines became increasingly sensitive to EZP011989 with EZH2 overexpression. (**c**) *BAP1*-mutant cells became less invasive when treated with the EZH2 inhibitor GSK126. (**d**) E-Cadherin expression increased in the cell line H226 following treatment with GSK126.

1. Lara-Astiaso, D., *et al.* Immunogenetics. Chromatin state dynamics during blood formation. *Science* **345**, 943-949 (2014).